

## EFFICIENT NUMERICAL METHODS FOR THE KDV EQUATION

MI-YOUNG KIM<sup>†</sup> AND YOUNG-KWANG CHOI

DEPARTMENT OF MATHEMATICS, INHA UNIVERSITY, INCHEON 402-751, KOREA

*E-mail address:* mikim@inha.ac.kr; effort8@hanmail.net

**ABSTRACT.** We consider the second order Strang splitting method to approximate the solution to the KdV equation. The model equation is split into three sets of initial value problems containing convection and dispersal terms separately. TVD MUSCL or MUSCL scheme is applied to approximate the convection term and the second order centered difference method to approximate the dispersal term. In time stepping, explicit third order Runge-Kutta method is used to the equation containing convection term and implicit Crank-Nicolson method to the equation containing dispersal term to reduce the CFL restriction. Several numerical examples of weakly and strongly dispersive problems, which produce solitons or dispersive shock waves, or may show instabilities of the solution, are presented.

### 1. INTRODUCTION

The deep water wave has to be considered to design harbor structure in coastal region. As waves enter into a region of shallow water, they are transformed by shoaling, refraction, diffraction, reflection and they affect to the harbor structure. The development of wave numerical model has to be preceded to use the deep water wave height for designing harbor structure in coastal region.

On the other hand, the nonlinearity and dispersion have to be contained in the governing equation to simulate deep water wave and wave transformation in shallow water. The simplest equation to simulate both wave nonlinearity and dispersion is Korteweg de Vries (KdV) equation in one dimensional space, which is given as follows:

$$\begin{aligned} \frac{\partial u}{\partial t} + \frac{\partial f(u)}{\partial x} + \varepsilon \frac{\partial^3 u}{\partial x^3} &= 0, & t > 0, & \quad x \in R, \\ u(x, 0) &= u_0(x), & x \in R, \end{aligned} \quad (1.1)$$

where  $u$  denotes the solution,  $f(u) = \alpha u^2$ ,  $\alpha$  and  $\varepsilon$  are constants, and  $u_0$  is a given function in  $BV$ .

---

Received by the editors September 13, 2011; Revised November 20, 2011; Accepted in revised form December 13, 2011.

*Key words and phrases.* KdV equation, Strang splitting, MUSCL, TVD, Crank-Nicolson.

This work was supported by BSRP through the NRF of Korea funded by the Ministry of Education, Science and Technology (C00099).

<sup>†</sup> Corresponding author.

In this paper, we study the numerical methods to approximate the solution to (1.1). We consider weakly and strongly dispersive problems. We are particularly interested in high order approximations in space and time. The solution to the weakly dispersive problems may be physically oscillatory. Sometimes instability of the solution occurs and/or solitons are produced. In the strongly dispersive problems, a soliton can propagate with balance between non-linearity of the convection and high order dispersion as time evolves.

In time integration, the explicit scheme for the dispersal equation requires a restrictive CFL condition. In order to loose such a restrictive condition, we consider the second order Strang splitting method which treats the convective term and dispersal term separately. More precisely, we apply the explicit third order Runge-Kutta method to the nonlinear convection equation and the implicit Crank-Nicolson method to the third order dispersal equation.

In space discretization, we apply the finite volume method of MUSCL (Monotone Upstream Central) type to the nonlinear convection equation. When the initial condition is smooth and the solution is smooth, the MUSCL scheme without TVD (Total variation diminishing) is more efficient than the TVD MUSCL scheme. When the initial condition is discontinuous, the TVD MUSCL scheme removes the spurious oscillation.

Most schemes developed so far, for the KdV equations, are FDMs (finite difference methods) and the methods based on FDM such as narrow box schemes, symplectic and multisymplectic methods. We refer the readers to [1, 2, 4, 11] and the references cited therein for more details. High order FVM or FDM combined with high order time discretization may produce instability in the solution. One of the main concern of this article is to provide a high order scheme in space and time with relaxed CFL condition.

Very recently, an LDG(local discontinuous Galerkin) method was introduced by Yan and Shu [11]. There, two auxiliary variables were introduced to approximate the third order dispersal term and discontinuous Galerkin (DG) method was applied to the system of the resulting equation. In time integration, explicit third order Runge-Kutta method [3] was used and very small time step was used in their approach.

In this paper, we loose the CFL condition. More precisely, we consider a semi-explicit time stepping by introducing second order Strang splitting. The restrictive CFL condition due to high order dispersal term is then relaxed only to the convection term. We show that the resulting numerical solution is stable. By TVD MUSCL, we also remove spurious wiggles near the discontinuities of the dispersive shock wave.

The organization of the paper is given as follows. In section 2, we introduce the finite volume method to approximate the Burger's equation. In section 3, we describe the Strang splitting and time stepping methods. In section 4, we present some numerical examples of weakly and strongly dispersive problems, which produce solitons or dispersive shock waves. Instabilities of the solution may also occur. Finally, in section 5, we give some concluding remarks.

## 2. FINITE VOLUME METHOD

In this section, we consider the following hyperbolic conservation law:

$$\begin{aligned} \frac{\partial u}{\partial t} + \frac{\partial f(u)}{\partial x} &= 0, & t > 0, & -1 \leq x < 1, \\ u(x+1, t) &= u(x, t), & t > 0, \\ u(x, 0) &= u_0(x), & -1 \leq x < 1, \end{aligned} \quad (2.1)$$

where  $f(u) = \alpha u^2$ .

A finite volume discretization to (2.1) is then obtained by taking the integral to (2.1) over the cell  $I_i = [x_{i-1/2}, x_{i+1/2}]$ .

$$\frac{d}{dt} \bar{u}_i(t) = -\frac{1}{\Delta x} \{f(u(x_{i+1/2}, t)) - f(u(x_{i-1/2}, t))\}, \quad (2.2)$$

where  $\Delta x = x_{i+1/2} - x_{i-1/2}$  and  $\bar{u}_i(t) = \frac{1}{\Delta x} \int_{x_{i-1/2}}^{x_{i+1/2}} u(x, t) dx$  represents cell-averaged value on the cell  $I_i$ .

We now integrate (2.2) over  $[t^n, t^{n+1}]$  and apply Euler forward time stepping method to get

$$\bar{u}_i^{n+1} = \bar{u}_i^n - \frac{\Delta t}{\Delta x} (\hat{f}_{i+1/2}^n - \hat{f}_{i-1/2}^n), \quad (2.3)$$

where  $\hat{f}_{i+1/2}^n = \frac{1}{\Delta t} \int_{t^n}^{t^{n+1}} f(u(x_{i+1/2}, t)) dt$  is the approximation to the physical flux  $f(u)$  of (2.1) and is called the numerical flux at the cell interface  $x_{i+1/2}$ . The numerical flux should be then determined to obtain the approximate solution in next time step.

Meanwhile, it is well known that solutions of (2.1) may develop discontinuities in finite time even when the initial data are smooth. A simple class of flux functions  $\hat{f}$ , for which (2.3) converges, for all  $f$ , to the unique entropy solution in  $L^\infty(L^1(R); [0, T])$ , as  $\Delta x \rightarrow 0$ , for any  $T > 0$ , is the class of  $E$  schemes. It is clear that this class includes the widely known class of monotone schemes. One particular monotone scheme is due to Godunov. However  $E$  schemes are at most first order accurate [7] and the first order accurate schemes give poor resolution in many problems. On the other hand, high order schemes produce spurious oscillations at the discontinuities of the solution. These spurious oscillations will happen in finite difference and finite element methods [5], finite volume methods [10] without special treatment.

In this paper, we consider TVD schemes which produce oscillation free solutions and high accuracy. A scheme is called TVD if it satisfies the following:

$$\begin{aligned} TV(u^{n+1}) &\leq TV(u^n), & \forall n, \\ TV(u^n) &= \sum_{i=-\infty}^{\infty} |u_{i+1}^n - u_i^n|. \end{aligned}$$

TVD scheme is thus stable. The readers refer to [6] and [10] for more details on TVD schemes.

**2.1. MUSCL scheme.** The MUSCL scheme is a second order accurate extension of Godunov's method. The first step in MUSCL is the reconstruction of a piecewise linear description of the solution. In the interval  $I_i$  the result of this operation is

$$\tilde{u}^n(x, t_n) = \bar{u}_i^n + (x - x_i)\sigma_i^n, \quad (2.4)$$

where  $\bar{u}_i^n$  is the cell-averaged value and  $\sigma_i^n$  is the slope function. If we choose the downwind slope

$$\sigma_i^n = \frac{\bar{u}_{i+1}^n - \bar{u}_i^n}{\Delta x} \quad (2.5)$$

as the slope function, the method reduces to the Lax-Wendroff method.

TVD MUSCL schemes use slope limiters which reduce spurious oscillations at the discontinuities of the solution. In this paper, we consider the MC (monotonized central-difference) limiter as the slope function:

$$\sigma_i^n = \minmod\left(\frac{\bar{u}_{i+1}^n - \bar{u}_{i-1}^n}{2dx}, \minmod\left(2\left(\frac{\bar{u}_i^n - \bar{u}_{i-1}^n}{dx}\right), 2\left(\frac{\bar{u}_{i+1}^n - \bar{u}_i^n}{dx}\right)\right)\right),$$

$$\minmod(a, b) = \frac{\text{sign}(a) + \text{sign}(b)}{2} \min(|a|, |b|).$$

The next step of the MUSCL is the computation of the numerical flux at the cell interface by solving the Riemann problem with extrapolated values obtained from the reconstruction. Here we consider the Godunov scheme and the Roe scheme. In Godunov scheme the numerical flux at the interface is computed by solving the Riemann problem exactly. The Godunov scheme is simplified as follows.

$$\begin{aligned} \hat{f}_{i+1/2}^{Godunov} &= f(u(x_{i+1/2}, t^n)) \\ &= \begin{cases} \min_{u \in [u_i, u_{i+1}]} f(u), & u_i \leq u_{i+1}, \\ \max_{u \in [u_i, u_{i+1}]} f(u), & u_i > u_{i+1}. \end{cases} \end{aligned}$$

In Roe scheme the numerical flux is computed by the approximate Riemann solver, where the nonlinear term of conservation law is linearized. Roe scheme is simpler than Godunov scheme and is applied to the system of the conservation law more easily. Roe flux is given as follows [9]:

$$\hat{f}_{i+1/2}^{Roe} = \frac{f_i + f_{i+1}}{2} - \frac{1}{2} |\bar{u}_{i+1/2}| (u_{i+1} - u_i),$$

$$\bar{u}_{i+1/2} = \begin{cases} \frac{1}{2}(u_i + u_{i+1}), & u_i \neq u_{i+1}, \\ u_i, & u_i = u_{i+1}. \end{cases}$$

It is known that the solution of the TVD MUSCL to (2.1) satisfies the entropy inequality with the approximate entropy flux (1.20) in [8]. The solution of the TVD MUSCL thus converges to the unique solution of (2.1) provided the initial data is in  $BV$ .

It is also known [8] that TVD MUSCL and MUSCL schemes are second order accurate provided the solution of (2.1) is smooth.

## 3. SPLITTING METHOD

The CFL condition to obtain a stable approximate solution to (1.1) by an explicit method is very restrictive in general. The CFL condition in (1.1) by a finite difference method, for example, is given by [1]

$$\Delta t < \Delta x / \left[ \frac{|\varepsilon|}{\Delta x^2} + 2|\alpha u_{max}| \right].$$

In [11], small time step is also needed to the KdV equations. In this paper we consider second order accurate Strang splitting method to avoid small time step restriction due to the third order dispersal term. The convection and the third order dispersal terms are split into a pair of initial value problems. The split form is then given by the following:

$$\left. \begin{array}{l} PDE : \frac{\partial u}{\partial t} + \frac{\partial f(u)}{\partial x} = 0, \quad f(u) = \alpha u \\ IC : u(x, t^n) = u^n \end{array} \right\} \implies \bar{u}^{n+1} \quad (3.1)$$

$$\left. \begin{array}{l} PDE : \frac{\partial u}{\partial t} + \varepsilon \frac{\partial^3 u}{\partial x^3} = 0 \\ IC : \bar{u}^{n+1} \end{array} \right\} \implies \bar{u}^{n+2} \quad (3.2)$$

$$\left. \begin{array}{l} PDE : \frac{\partial u}{\partial t} + \frac{\partial f(u)}{\partial x} = 0, \quad f(u) = \alpha u \\ IC : \bar{u}^{n+2} \end{array} \right\} \implies u^{n+1} \quad (3.3)$$

The result of (3.1)-(3.3) can be expressed as the form of

$$u^{n+1} = C^{(\frac{1}{2}\Delta t)} D^{\Delta t} C^{(\frac{1}{2}\Delta t)}(u^n).$$

One may interpret  $C^{(\frac{1}{2}\Delta t)}$  as the solution operator for (3.1) and (3.3) with time step  $\frac{1}{2}\Delta t$  and  $D^{\Delta t}$  as the solution operator for (3.2) with time step  $\Delta t$ . We apply the MUSCL scheme to approximate the flux term of (3.1) and (3.3). For time stepping, we apply the explicit third order Runge-Kutta method [3]:

$$\begin{aligned} u^{(1)} &= u^n + \Delta t L(u^n), \\ u^{(2)} &= \frac{3}{4}u^n + \frac{1}{4}u^{(1)} + \frac{1}{4}\Delta t L(u^{(1)}), \\ u^{n+1} &= \frac{1}{3}u^n + \frac{2}{3}u^{(2)} + \frac{2}{3}\Delta t L(u^{(2)}), \end{aligned} \quad (3.4)$$

where  $L(u) = -f(u)_x$ .

For the approximation of (3.2), we use the second order centered difference method in space and Crank-Nicolson method in time, which is implicit and unconditionally stable. The scheme for (3.2) is then expressed as follows:

$$\begin{aligned} \frac{\bar{u}_i^{n+1} - \bar{u}_i^n}{\Delta t} &= \frac{1}{2}(-\varepsilon) \left\{ \frac{\bar{u}_{i+2}^{n+1} - 2\bar{u}_{i+1}^{n+1} + 2\bar{u}_{i-1}^{n+1} - \bar{u}_{i-2}^{n+1}}{2\Delta x^3} \right. \\ &\quad \left. + \frac{\bar{u}_{i+2}^n - 2\bar{u}_{i+1}^n + 2\bar{u}_{i-1}^n - \bar{u}_{i-2}^n}{2\Delta x^3} \right\} \end{aligned} \quad (3.5)$$

or it is rewritten as

$$a\bar{u}_{i-2}^{n+1} + b\bar{u}_{i-1}^{n+1} + c\bar{u}_i^{n+1} + d\bar{u}_{i+1}^{n+1} + e\bar{u}_{i+2}^{n+1} = F_i^n, \quad i = 1, \dots, ncells, \quad (3.6)$$

where  $a = -\frac{\varepsilon\Delta t}{4\Delta x^3}$ ,  $b = \frac{\varepsilon\Delta t}{2\Delta x^3}$ ,  $c = 1$ ,  $d = -b$ ,  $e = -a$ ,  $F_i^n = e\bar{u}_{i-2}^n + d\bar{u}_{i-1}^n + c\bar{u}_i^n + b\bar{u}_{i+1}^n + a\bar{u}_{i+2}^n$ , and  $ncells$  denotes the number of cells.

By considering a periodic boundary condition, we thus obtain the matrix form of

$$\begin{pmatrix} c & d & e & 0 & 0 & \cdots & 0 & 0 & a & b \\ b & c & d & e & 0 & \cdots & & 0 & 0 & a \\ a & b & c & d & e & 0 & 0 & \cdots & 0 & 0 \\ 0 & a & b & c & d & e & 0 & \cdots & 0 & 0 \\ & & & & \vdots & & & & & \\ 0 & 0 & 0 & 0 & 0 & a & b & c & d & e \\ e & 0 & 0 & 0 & 0 & 0 & a & b & c & d \\ d & e & 0 & 0 & 0 & 0 & 0 & a & b & c \end{pmatrix} \begin{pmatrix} u_1^{n+1} \\ u_2^{n+1} \\ u_3^{n+1} \\ u_4^{n+1} \\ \vdots \\ u_{ncells-2}^{n+1} \\ u_{ncells-1}^{n+1} \\ u_{ncells}^{n+1} \end{pmatrix} = \begin{pmatrix} F_1^n \\ F_2^n \\ F_3^n \\ F_4^n \\ \vdots \\ F_{ncells-2}^n \\ F_{ncells-1}^n \\ F_{ncells}^n \end{pmatrix},$$

where  $u_{-1}^n = u_{ncells-1}^n$ ,  $u_0^n = u_{ncells}^n$ ,  $u_{ncells+1}^n = u_1^n$ , and  $u_{ncells+2}^n = u_2^n$ .

We apply the ILU decomposition to solve the matrix equation. The matrix is then decomposed to L and U part before the time stepping because the matrix is constant in time and it does not take much time to solve matrix equation.

#### 4. NUMERICAL RESULTS

In this section we present several numerical examples to see the possibility of the application to diverse problems. We study the behavior of the numerical solutions to weakly and strongly dispersive problems, instabilities of the solutions, and the efficiency for the long time computation of the solitons. We compare the results with ones of [11], [1], and [4]. We use smooth initial conditions in Examples 4.1 - 4.6, while we use a discontinuous initial condition in Example 4.7. We apply both Godunov and Roe schemes in Example 4.7, while we apply Godunov scheme in Examples 4.1 - 4.6.

In the approximation of the convection term, we apply the second order accurate MUSCL scheme when the initial condition is smooth and TVD MUSCL when the initial condition is discontinuous. In the approximation of the dispersal term, we apply the second order centered difference method. On the other hand, Yan and Shu [11] applied LDG method with  $P^2$  element. The number of cell required to model the wave dispersion in Example 4.1 is larger than the one of Yan and Shu [11] due to the lower order approximation. However, the number of cell required in the computation of the solution to problem of the zero dispersion limit in Example 4.2, is less than the one of Yan and Shu [11]. The third order dispersal term and the first order convection terms are split by Strang splitting method. Requirement of the time step size, which is restrictive in Yan and Shu [11], can be relaxed by using Crank-Nicolson scheme to (3.2).

Throughout Examples 4.1 - 4.3, we present numerical results of the soliton propagation. Soliton propagates with balance between nonlinearity and dispersion. Thus precise computation is needed on the evaluation of the nonlinear convection and the dispersion terms.

$\Delta x$	$E_{max}$	$C_{max}$
0.08	0.315492163	1.649529193
0.04	0.100561284	2.042278843
0.02	0.024414263	2.023482311
0.01	0.006005024	2.040861876
0.005	0.001459332	1.982782879
0.0025	0.000369213	1.993765419

TABLE 1. Convergence estimates for single soliton example.

**Example 4.1.** In this example, we solve (2.1) with initial condition of single soliton:

$$u_0(x) = 3c \operatorname{sech}^2(k(x - x_0)), \quad (4.1)$$

$$c = 0.3, \quad x_0 = 0.5, \quad k = (1/2)\sqrt{(c/\varepsilon)}, \quad \varepsilon = 5 \times 10^{-4},$$

with  $\alpha = 0.5$  in (1.1). The soliton is located at  $x=0.5$  at  $t=0$  with amplitude of 0.9. We impose periodic boundary condition. We see that the exact solution is given [2] by

$$u(x, t) = 3c \operatorname{sech}^2(k(x - ct - x_0)).$$

The computation is done over  $0 < x < 2$  and  $0 < t \leq 3$  with  $\Delta x = 0.01$  (and thus 200 cells) and  $\Delta t = 0.02$ . The results are presented in Figure 1. The soliton propagates while maintaining the initial amplitude and the velocity  $c$  as seen in Figure 1.

We also compute the order of convergence of the approximate solution by  $L_\infty$  norm:

$$E_{\max}(\Delta x) = \max_{i \geq 1} |u_i^h(t) - u_i(t)|, \quad (t = 0.5),$$

$$C_{\max} = \frac{\log \frac{E_{\max}(\Delta x)}{E_{\max}(\Delta x/2)}}{\log 2},$$

where  $u_i^h$  and  $u_i$  denote numerical and exact solutions, respectively. Convergence results are given in Table 1. We see, from Table 1, that the numerical solution converges with the rate of order 2.

**Example 4.2.** In this example, we study the double soliton collision problem. The initial condition is given by

$$u_0(x) = 3c_1 \operatorname{sech}^2(k_1(x - x_1)) + 3c_2 \operatorname{sech}^2(k_2(x - x_2)),$$

$$c_1 = 0.3, \quad c_2 = 0.1, \quad x_1 = 0.4, \quad x_2 = 0.8,$$

$$k_i = (1/2)\sqrt{(c_i/\varepsilon)}, \quad (\text{for } i = 1, 2), \quad \varepsilon = 4.84 \times 10^{-4},$$

with  $\alpha = 0.5$  in (1.1). The soliton is located at  $x=0.4$  and  $x=0.8$  at  $t=0$  with the amplitudes of 0.9 and 0.3, respectively. Periodic boundary condition is imposed. The computation is done over  $0 < x < 2$  and  $0 < t \leq 4$  with  $\Delta x=0.01$  (and thus 200 cells) and  $\Delta t=0.02$ . The results are

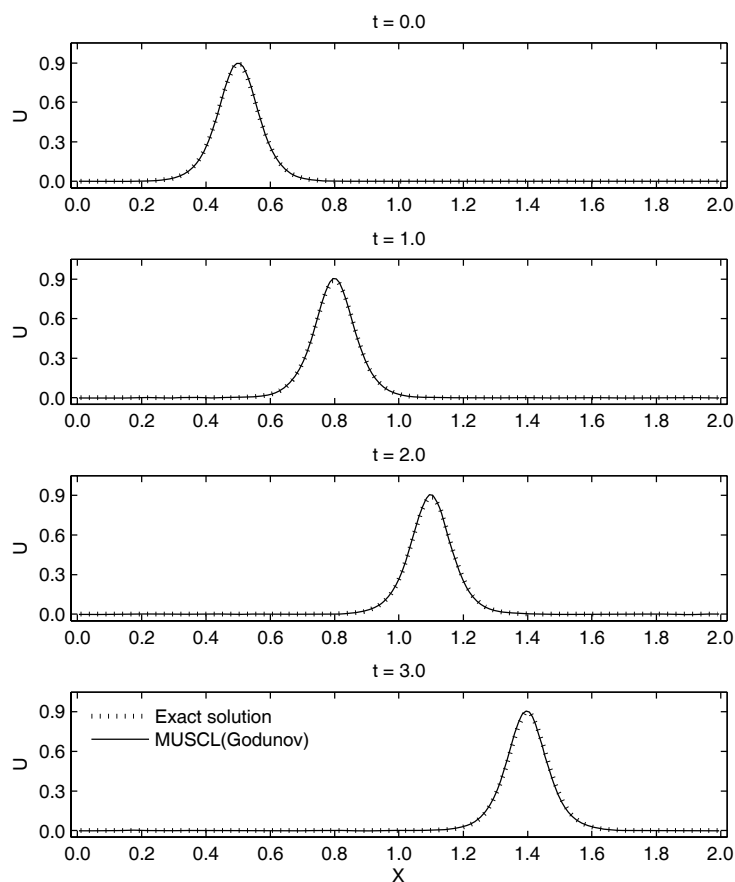


FIGURE 1. Comparison of spatial profile of solitons : snapshots of solution profile between numerical solution and analytical solution.

presented in Figure 2. Solitons pass through each other and the shape and the velocity of each soliton are kept. The phase lag gradually develops between bigger soliton and smaller soliton as  $t$  evolves after two solitons collide each other at  $t=1$ . These solitons retain their shapes after interaction.

**Example 4.3.** In this example, we study the triple soliton splitting problem. The initial condition is given by

$$u_0(x) = \frac{2}{3} \operatorname{sech}^2\left(\frac{x-1}{\sqrt{(108\varepsilon)}}\right), \quad \varepsilon = 10^{-4},$$



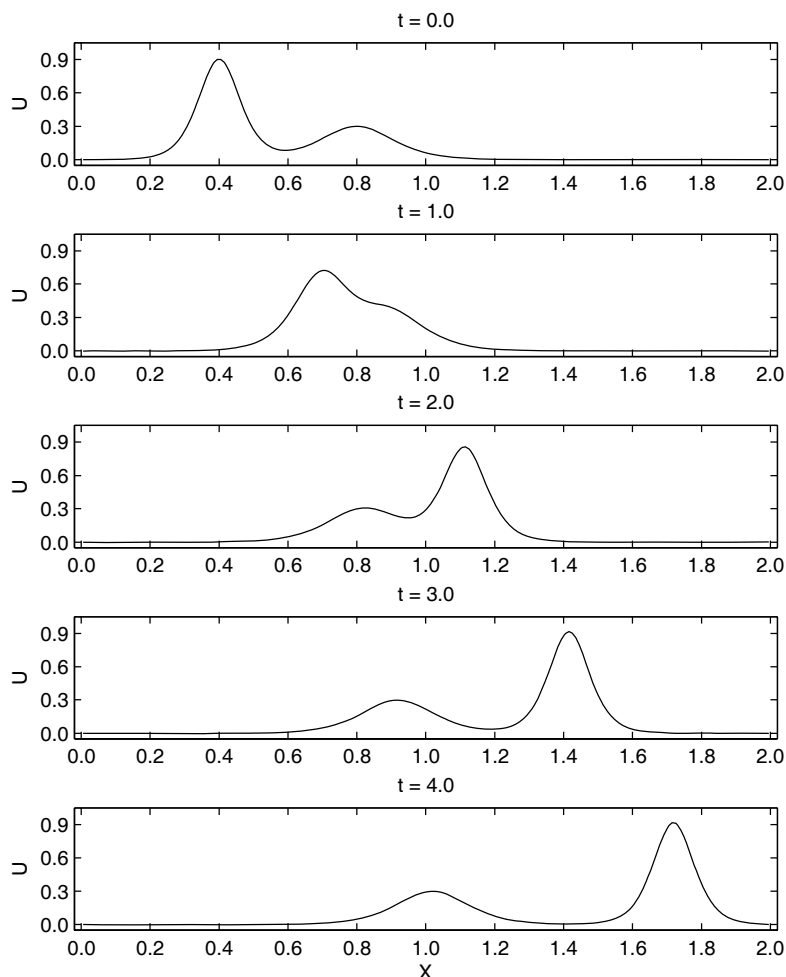


FIGURE 2. Snapshots of double soliton collision case.

with  $\alpha = 0.5$  in (1.1). The soliton is located at  $x=1.0$ . Periodic boundary condition is imposed. The computation is done over  $0 < x < 3$  and  $0 < t \leq 4$  with  $\Delta x = 0.01$  (and thus 300 cells) and  $\Delta t = 0.01$ . The results are presented Figure 3. The soliton is split into three components which have their own amplitudes as  $t$  evolves. Three solitons propagate while retaining their amplitudes as seen in Figure 3.

In Example 4.4, we compare the computation with the one of Yan and Shu [11]. Our computation is done with  $\Delta x = 0.01$  and  $\Delta t = 0.02$  or  $\Delta t = 0.01$  while the computation was done with  $\Delta x = 0.02$  and smaller  $\Delta t$  in [11]. We here note that their method is third order accurate in space and time, while our method is second order accurate.

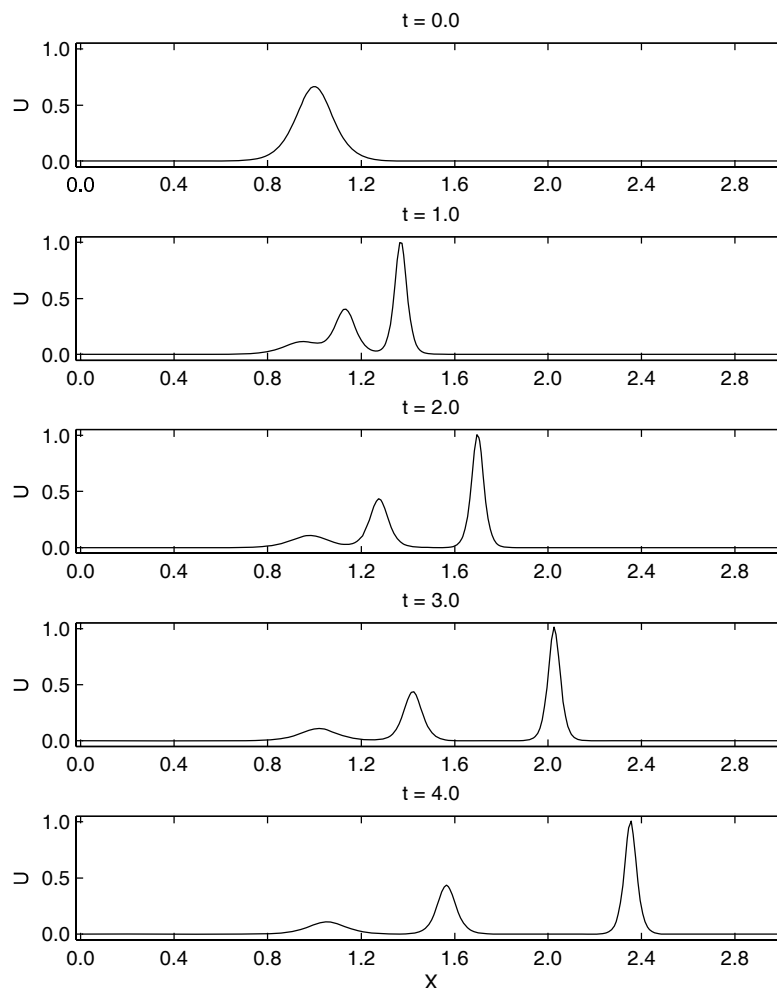


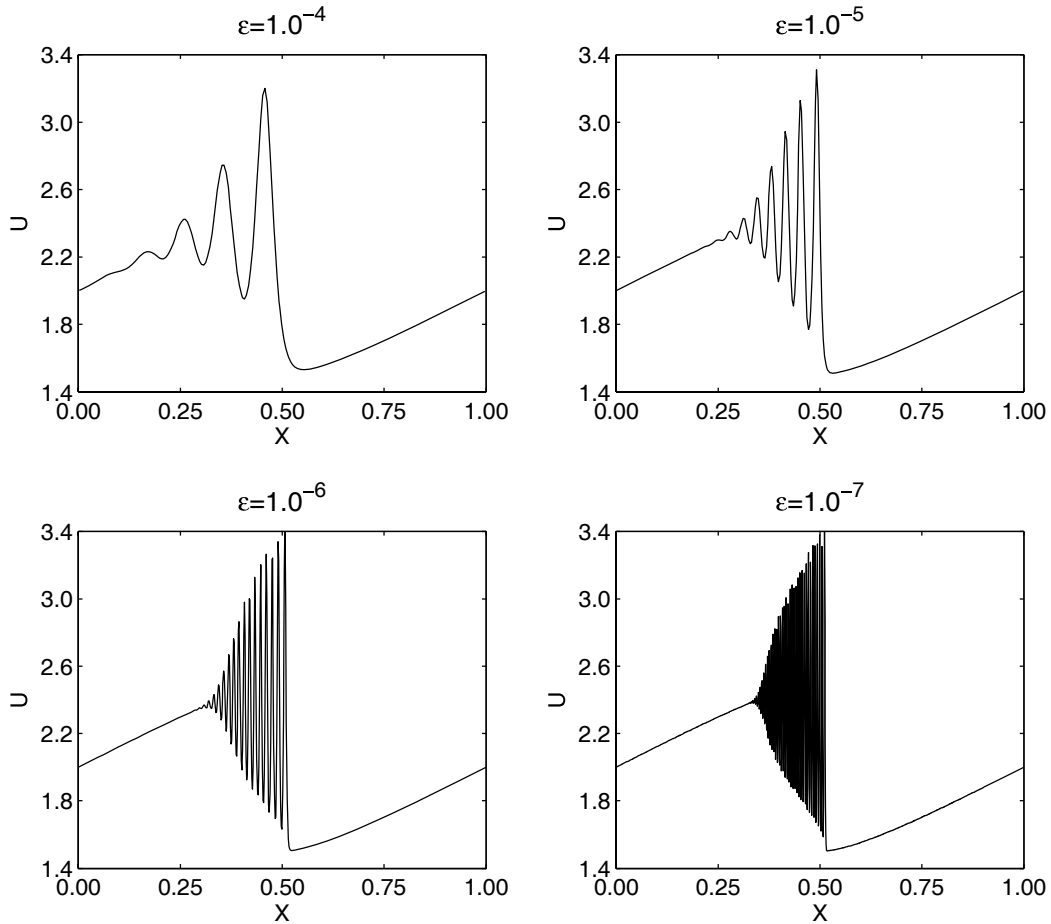
FIGURE 3. Snapshots of triple soliton splitting case.

**Example 4.4.** In this example, we study the case of zero dispersion limit. We solve (1.1) when  $\varepsilon$  is  $10^{-4}$ ,  $10^{-5}$ ,  $10^{-6}$ , and  $10^{-7}$ . The initial condition is given by

$$u_0(x) = 2 + 0.5 \sin(2\pi x) \quad (4.2)$$

with  $\alpha = 0.5$ . Periodic boundary condition is imposed. The computation is done over  $0 < x < 1$  and  $0 < t < 0.5$ .

At the beginning, a sine function is placed but physical oscillation or dispersive shock wave pattern develops for each  $\varepsilon$  as time evolves. The results are presented in Figure 4.

FIGURE 4. Snapshots for each  $\varepsilon$  of Example 4.4.

We compare the computation with the one of [11]. We use 200 cells ( $\Delta x = 0.005$ ) and  $\Delta t = 0.005$  for  $\varepsilon = 10^{-4}$ , 300 cells ( $\Delta x = 0.0033$ ) and  $\Delta t = 0.002$  for  $\varepsilon = 10^{-5}$ , 650 cells ( $\Delta x = 0.0015$ ) and  $\Delta t = 0.000307$  for  $\varepsilon = 10^{-6}$ , and 1600 cells ( $\Delta x = 0.0006$ ) and  $\Delta t = 0.000125$  for  $\varepsilon = 10^{-7}$ , while Yan and Shu in [11] used  $P^2$  element with 300 cells for  $\varepsilon = 10^{-4}$  and  $10^{-5}$ , 800 cells for  $\varepsilon = 10^{-6}$  and 1700 cells for  $\varepsilon = 10^{-7}$ . They used much smaller  $\Delta t$  in all computations due to the CFL restriction. Our results which are obtained even by lower order schemes, are better. It was also seen that the maximum value of  $u$  at  $t = 0.5$  in [11] is smaller than that of ours given in Figure 4, when  $\varepsilon = 10^{-7}$ .

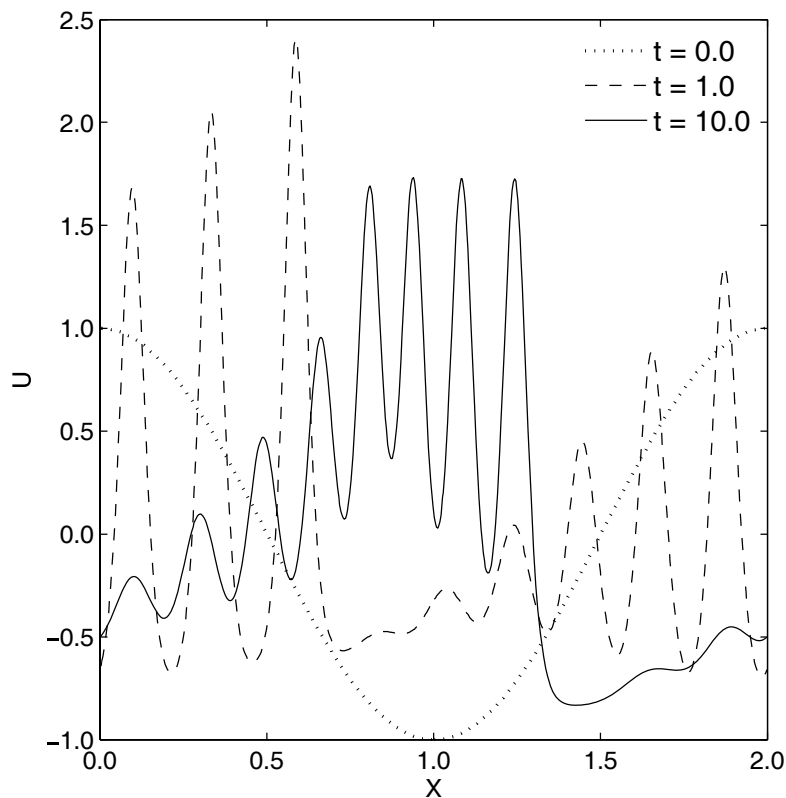


FIGURE 5. Numerical solution profile of Example 4.5.

**Example 4.5.** In this example, we study instabilities of the solution to (1.1). The initial condition is given by

$$u_0(x) = \cos(\pi x) \quad (4.3)$$

with  $\alpha = 0.5$  and  $\varepsilon = 4.84 \times 10^{-4}$ . Periodic boundary condition is imposed. The computation is done over  $0 < x < 2$  and  $0 < t \leq 10$  with  $\Delta x = 0.0033$  (600 cells) and  $\Delta t = 0.0015$ . The results are presented in Figure 5. At the beginning a cosine function is placed but the solution is split into solitons by dispersion and they propagate as time evolves. Asher and McLachlan [1] applied the narrow box scheme and showed rough resolutions. They used  $\Delta x = 0.02$  and  $\Delta t = 0.004$ . Here we use  $\Delta x = 0.01$  and  $\Delta t = 0.003$  to compare the results with [1]. The results are depicted in Figure 5-6.

**Example 4.6.** In this example, we study a strongly dispersive problem. We solve (1.1) with  $\alpha = 3$  and  $\varepsilon = 1$ . The initial condition is given by

$$u_0(x) = 6 \operatorname{sech}^2(x). \quad (4.4)$$

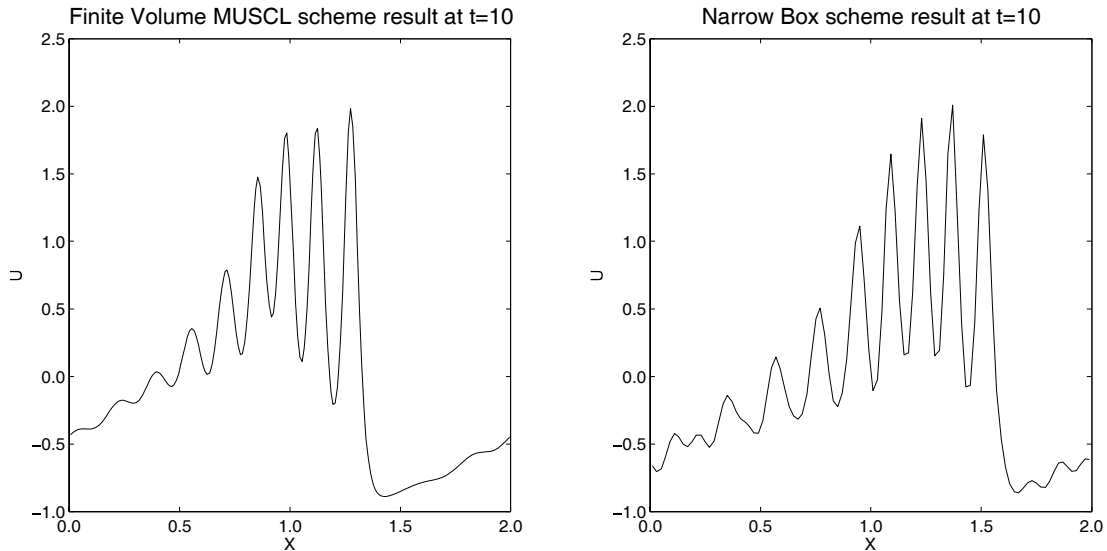


FIGURE 6. Comparison with narrow box scheme result on rough grid of Example 4.5.

The soliton is located at  $x=0$  and at  $t=0$ . Periodic boundary condition is imposed. The computation is done over  $-20 < x < 20$  and  $0 < t \leq 100$  with  $\Delta x = 0.03636$  (1100 cells) and  $\Delta t = 0.0001$ . The initial soliton is split into two components which have their own amplitude and propagate as time evolves. The results are presented in Figure 7.

In Example 4.6, Ascher and McLachlan [1] applied the semi-explicit and symplectic method, while they applied the narrow box scheme in Example 4.5. They used  $\Delta x = 0.05$  and  $\Delta t = 0.001$ .

**Example 4.7.** In this example, we study the problem of dispersive shock wave with discontinuous initial condition. We solve (1.1) with  $\alpha = 0.5$  and  $\varepsilon = 10^{-3}$ . The initial condition is given by

$$u(x, 0) = \begin{cases} 1, & x \leq 0, \\ 0, & x > 0. \end{cases}$$

The computation is done with  $\Delta x = 0.00625$  and  $\Delta t = 0.00625$ . We apply both TVD MUSCL and MUSCL schemes on the convection term. We also apply both Godunov and Roe schemes on the numerical flux. The results are similar and only the results of the Roe scheme are presented in Figures 8 - 9. The approximation of the MUSCL shows spurious wiggles near the discontinuity of the initial condition. They propagate to the left and are getting smaller as time evolves. On the other hand, the approximate solution of TVD MUSCL shows no spurious oscillation. The wavelength of oscillation, leading edge amplitude, and speed of the approximate solution of the TVD MUSCL agree well with the one of Hoefer et al. [4].

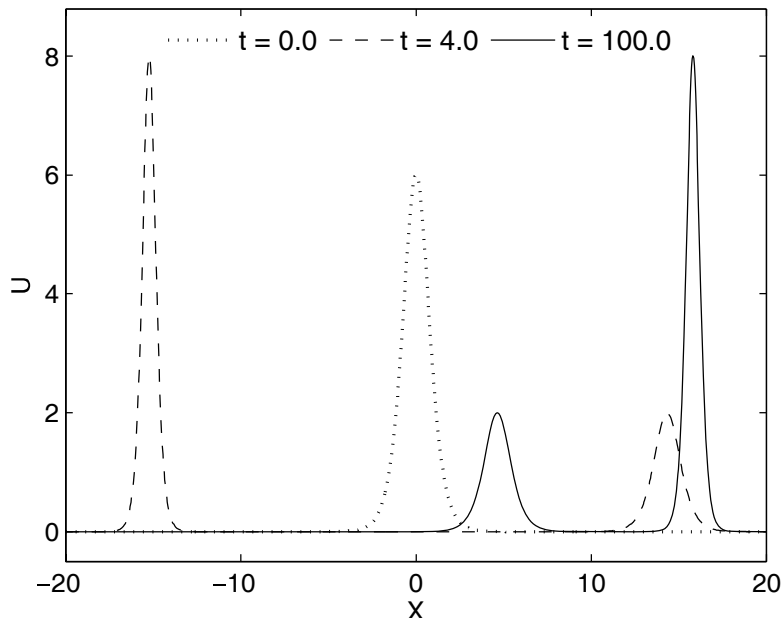


FIGURE 7. Numerical solution profile of Example 4.6.

## 5. CONCLUDING REMARKS

KdV equation shows very diverse behaviors in the solution depending on the values of the parameters. In weakly dispersive problems, spurious oscillations may occur in the numerical solutions. In strongly dispersive problems, solitons with their own amplitudes should be preserved for a long time. Instability of the solution may occur. Dispersive shock waves may also develop under discontinuous initial conditions. Due to high order dispersal term, the KdV equation usually requires small time step with restricted CFL condition for stability of the numerical solution. For the KdV equation, it is thus important to develop a high order scheme combined with high order time discretization, which is efficient for long time computation and for the computation requiring small time step size.

In this paper, Strang splitting method is applied to solve the KdV equations. The convection and the dispersal terms are split into a pair of initial value problems. The Crank-Nicolson scheme is applied to the equation containing third order derivative term to avoid CFL restriction. The MUSCL and the TVD MUSCL schemes are applied to the equation containing convection term.

Computations through Examples 4.1 - 4.6 show that the CFL restrictions are now relaxed in the methods: In Examples 4.1-4.3, the maximum of  $\Delta t/\Delta x$  is two. In Example 4.4, larger  $\Delta t$  and  $\Delta x$  than those of [11] are applicable. In Example 4.5, the maximum of  $\Delta t/\Delta x$  is 0.3, while the maximum of  $\Delta t/\Delta x$  in [1] is 0.2.

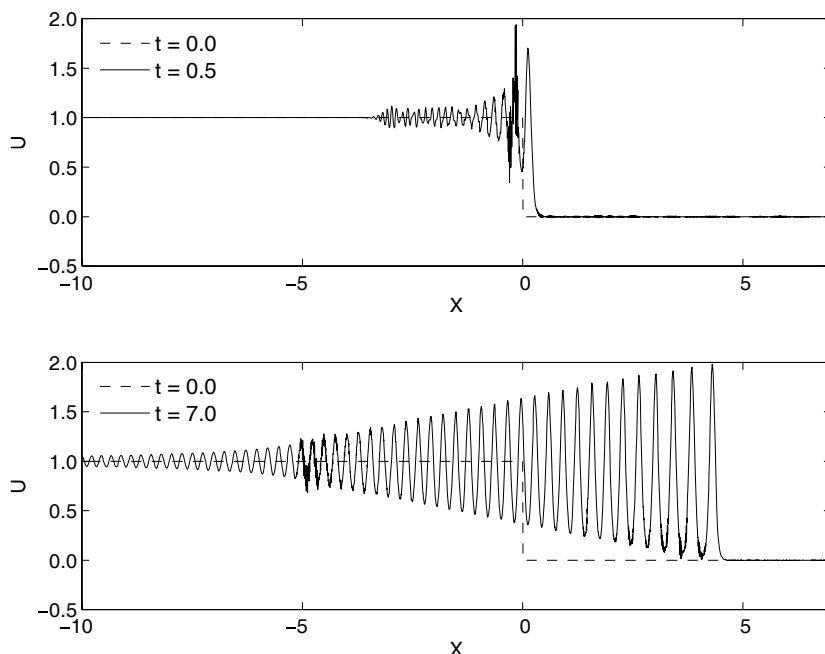


FIGURE 8. MUSCL scheme results of dispersive shock wave problem

In Example 4.7, TVD MUSCL and MUSCL schemes are applied to the dispersive shock wave problem. The approximate solution of the MUSCL scheme shows spurious wiggles. By TVD MUSCL we remove spurious wiggles. Resulting numerical solution agrees well with [4] in wavelength of oscillation, leading edge amplitude, and speed of the solution.

We expect that, in the approximation of the wave equations in Oceanography, non-physical oscillations which is developed at discontinuous depth, can be removed without restriction of small time step due to the high order dispersion term. Further research in this direction is an our ongoing work.

#### REFERENCES

- [1] U. M. Ascher and R. I. McLachlan, *On symplectic and Multisymplectic schemes for the KdV equation*, Journal of Scientific Computing **25**, (2005), 83–104.
- [2] K. Djidjeli, W. G. Price, E. H. Twizell and Y. Wang, *Numerical methods for the solution of the third- and fifth-order dispersive Korteweg-de Vries equations*, Journal of Computational and Applied Mathematics **58**, (1995), 307–336.
- [3] S. Gottlieb and C. -W. Shu, *Total variation diminishing Runge-Kutta schemes*, Mathematics of Computation **67**, (1998), no. 221, 73–85.
- [4] M. A. Hofer, M. J. Ablowitz, I. Coddington, E. A. Cornell, P. Engels and V. Schweikhard, *Dispersive and classical shock waves in Bose-Einstein condensates and gas dynamics*, Physical Review A **74**, (2006), 023623-1–023623-24.

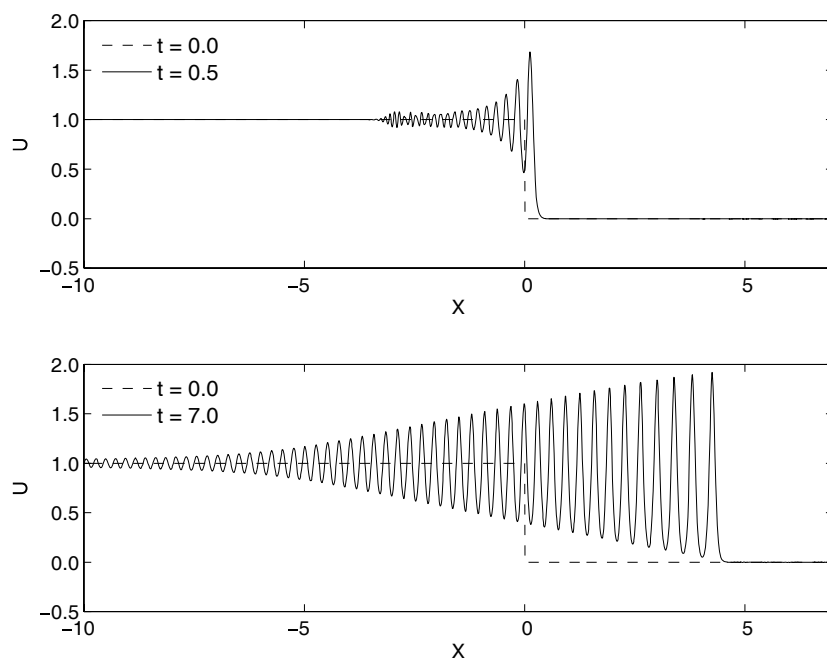


FIGURE 9. TVD MUSCL scheme results of dispersive shock wave problem

- [5] C. Johnson, *Numerical solution of partial differential equations by the finite element method*, Cambridge University Press, 1987.
- [6] R. J. Leveque, *Finite volume methods for hyperbolic problems*, Cambridge University Press, 2002.
- [7] S. Osher, *Riemann solvers, the entropy condition, and difference approximations*, *SIAM J. Numer. Anal.* **21**, (1984), no. 21, 217–235.
- [8] S. Osher, *Convergence of generalized MUSCL schemes*, *SIAM J. Numer. Anal.* **22**, (1985), no. 5, 217–235.
- [9] J. C. Tannehill, D. A. Anderson and R. H. Pletcher, *Computational fluid mechanics and heat transfer*, Taylor & Francis, 1997.
- [10] E. F. Toro, *Riemann solvers and numerical methods for fluid dynamics*, Springer, 1999.
- [11] J. Yan and C. -W. Shu, *A local discontinuous Galerkin method for KdV type equations*, *SIAM Journal on Numerical Analysis* **40**, (2002), no. 2, 769–791.